Macromolecules

ARTICLE

pubs.acs.org/Macromolecules

Well-Defined Amphiphilic Block Copolymers and Nano-objects Formed *in Situ* via RAFT-Mediated Aqueous Emulsion Polymerization

Xuewei Zhang,[†] Stéphanie Boissé,[†] Wenjing Zhang,[‡] Patricia Beaunier,[§] Franck D'Agosto,[‡] Jutta Rieger,[*,†] and Bernadette Charleux[*,‡]

[†]UPMC Sorbonne Universités and CNRS, Laboratoire de Chimie des Polymères, UMR7610, 3 Rue Galilée, Bat. Raphaël, 94200 Ivry sur Seine, France

[‡]Université de Lyon, Univ Lyon 1, CPE Lyon, CNRS UMR 5265, Laboratoire de Chimie Catalyse Polymères et Procédés (C2P2), LCPP, Bat 308F, 43 Bd du 11 novembre 1918, 69616 Villeurbanne, France

[§]Service commun de Microscopie Electronique ; Laboratoire de Réactivité de Surface (LRS), Sorbonne Universités UPMC and CNRS UMR 7197, 4 Place Jussieu, Bat. F 75252, Paris, France

Supporting Information

ABSTRACT: A hydrophilic poly(methacrylic acid-*co*-poly(ethylene oxide) methyl ether methacrylate) copolymer with a trithiocarbonate reactive group was used in the free-radical, batch emulsion polymerization of styrene. It allowed fast polymerizations and high final conversions to be achieved, and the parameters for a good control over the formation of well-defined amphiphilic diblock copolymers were identified. These diblock copolymers self-assembled *in situ* into nano-objects of various morphologies upon chain extension. Achieving a good control over the formed diblock copolymers was shown to be an important step toward a better understanding of the parameters that affect the shape and size of the self-assembled objects, the ultimate goal being the ability to predict and fine-tune them on purpose.

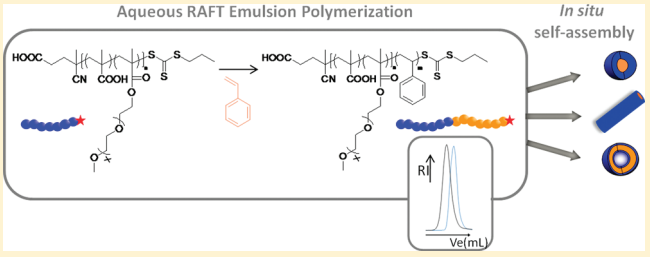

INTRODUCTION

Since the advent of controlled/living free-radical polymerization[1−4] (CRP) based on reversible deactivation of the propagating radicals,[5] considerable effort has been put in its development in aqueous emulsion polymerization.[6−13] Indeed, this process, which is used at a very large scale in the industry, offers many advantages over bulk or solution polymerization: large rates and high final conversions, low viscosity even at high concentrations, good control over exothermicity, absence of volatile organic compounds, easy recovery and manipulation of the products along with the possibility to use the polymer suspension directly in the final product. Besides these benefits in terms of polymerization reaction, the technique offers the unique advantage of leading to nanoparticles with large surface area and control over surface and volume composition and/or functionality. All of them contribute to the specific properties of the products. The development of CRP in aqueous emulsion[6−13] offers an additional feature, which is the control over the polymer architecture. For instance, phase separation of hydrophobic block copolymers within the particle cores has been explored.[14−17] Another particularly interesting possibility is the design of amphiphilic block copolymer core−shell nanoparticles formed by *in situ* chain extension of a hydrophilic living precursor polymer.[18−36] This method follows a polymerization-induced micellization mechanism and allows the development of self-stabilized particles, in the complete absence of surfactant. Large polymer concentrations can be achieved along with very small particle sizes, consistent with the formation of crew-cut micelle assemblies. Moreover, in a way similar to the postpolymerization self-assembling of amphiphilic block copolymers,[37−41] it was shown recently that various morphologies such as vesicles,[30,35] elongated micelles,[30,35] and nanofibers[35] could be reached directly via CRP in aqueous emulsion. RAFT dispersion polymerization in water[31] or methanol[42-44] is also a promising concept; in contrast to emulsion polymerization, the polymerization is then performed in a good solvent for the monomer but not for the forming polymer.

When studying block copolymer assemblies, the control over the polymerization (i.e., blocking efficiency and block lengths) is of crucial importance. It is thus similarly critical to achieve high structural quality in emulsion polymerization, when polymerization-induced micellization is targeted. The best CRP methods so far to synthesize amphiphilic block copolymers in emulsion polymerization were mainly NMP[22−25,28−30] (nitroxide-mediated polymerization) and RAFT[19−21,26,27,31−35] (reversible addition−fragmentation chain transfer). Their application was shown however to be less straightforward than anticipated. In NMP, using a poly(acrylic acid) macroalkoxyamine initiator,[22−25] the initiating efficiency was low and could be

Received: March 15, 2011
Revised: April 19, 2011
Published: May 06, 2011

Scheme 1. Schematic Representation of the One-Pot Synthesis of Amphiphilic Diblock Copolymer Assemblies by RAFT-Mediated Aqueous Emulsion Polymerization of Styrene in the Presence of Poly(methacrylic acid-*co*-poly(ethylene oxide) methyl ether methacrylate) MacroRAFT Agents

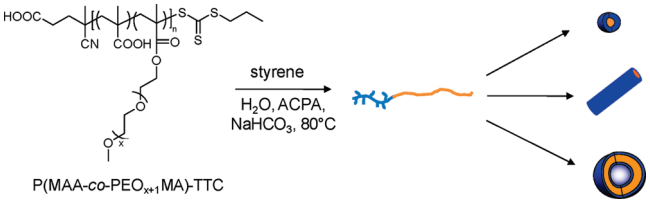

increased by using poly(methacrylic acid)-based macroinitiators.[28,29] In early works concerning RAFT emulsion polymerization and using a poly(acrylic acid)-based macromolecular RAFT agent (also called macroRAFT agent),[18,19,21,26] semicontinuous addition of the monomers was needed in order to reach control over chain growth along with good colloidal stability.[18−20] Later, it was shown that for a controlled RAFT-mediated emulsion polymerization in batch conditions a poly(ethylene oxide)-based trithiocarbonate precursor (PEO-TTC) led to very good control over the polymerization of *n*-butyl acrylate and its copolymerization with methyl methacrylate.[32,33] The results were however less satisfactory (low polymerization rates and broad molar mass distributions) for styrene.[32] They could be improved with the use of poly(*N*,*N*-dimethylacrylamide)[34] or poly(acrylic acid-*co*-poly(ethylene oxide) methyl ether acrylate) trithiocarbonate macroRAFT agents.[35] The latter allowed furthermore new particle morphologies to be achieved. Zhu et al.[45,46] studied the nucleation efficiency in the presence of poly(acrylic acid)-*b*-polystyrene amphiphilic oligomeric RAFT agents in the emulsion polymerization of styrene and showed that the pH was an important parameter.

With the purpose of targeting well-defined amphiphilic block copolymers via RAFT-mediated emulsion polymerization of styrene in simple batch conditions, we propose here a new system, which relies on the use of highly efficient macroRAFT agents (possessing high transfer constants). Those macroRAFT agents are random poly(methacrylic acid-*co*-poly(ethylene oxide) methyl ether methacrylate) copolymers with a trithiocarbonate reactive group (P(MAA-*co*-PEOMA)-TTC) (Scheme 1), which can be easily obtained in a single polymerization step. On this basis, our second purpose was to study the morphology of the *in situ* self-assembled amphiphilic block copolymers, from more conventional spherical particles to elongated micelles or vesicle-like structures. By varying the polymerization conditions, the styrene/macroRAFT agent ratio, and the structure of the macroRAFT agent, our goal was to explore the parameters allowing the aggregate morphologies to be tuned.

EXPERIMENTAL PART

Materials. 4,4′-Azobis(4-cyanopentanoic acid) (ACPA, >98%, Fluka), methacrylic acid (MAA, >99%, Fluka), poly(ethylene oxide) methyl ether methacrylate (PEO_8MA, M_n = 475 g/mol, >99% Aldrich and $PEO_{19}MA$, M_n = 950 g/mol, Aldrich), and the solvents 1,4-dioxane (100%, VWR GPR Rectapur) and tetrahydrofuran (THF, 99.9% for analysis from VWR Normapur) were used as received. Styrene (S, 99%, Aldrich) was distilled under reduced pressure before use. Deionized water was used for all emulsion polymerizations. 4-Cyano-4-(propylsulfanylthiocarbonyl) sulfanylpentanoic acid (CPP) was synthesized as reported before[47,48] (see ^{1}H NMR and ^{13}C NMR in the Supporting Information, Figure SI-1).

Synthesis of the Macromolecular RAFT Agent P(MAA-*co*-PEO_8MA)-TTC. A typical example for the procedure is as follows: MAA (2.58 g, 0.03 mol), PEO_8MA (14.25 g, 0.03 mol), CPP (237.2 mg, 0.86 mmol), ACPA (24.3 mg, 0.087 mmol), and 1,4-dioxane (14.31 g, 13.89 mL) were added into a 50 mL flask with a magnetic bar. 1,3,5-Trioxane (0.53 g, 5.86 mmol) was also added into the flask as an internal reference for determination of the monomer conversion by ^{1}H NMR. The solution in the septum-sealed flask was purged for 30 min with nitrogen and then heated to 70 °C in a thermostated oil bath under stirring. After 190 min, the polymerization was quenched by rapid cooling upon immersion of the flask in an iced water bath. The overall monomer molar conversion (46%) was determined by ^{1}H NMR spectroscopy in $CDCl_3$ by the relative integration of the protons of 1,3,5-trioxane at 5.0 ppm and the vinylic protons of monomers at 5.5 and 6.0 ppm. The polymer was purified by three precipitation/filtration cycles in diethyl ether at 0 °C and dried in a vacuum oven at room temperature. After methylation of the carboxylic acid groups with trimethylsilyldiazomethane,[49] it was further analyzed by size exclusion chromatography (SEC) in THF (experimental M_n: M_n^{LS} = 15 000 g/mol; M_w/M_n (PS calibration) = 1.16; dn/dc = 0.064 mL/g).

Synthesis of the Macromolecular RAFT Agent P(MAA-*co*-$PEO_{19}MA$)-TTC. A typical example for the procedure is as follows: MAA (1.29 g, 0.015 mol), $PEO_{19}MA$ (14.25 g, 0.015 mol), CPP (277.4 mg, 1.0 mmol), ACPA (28.0 mg, 0.100 mmol), and 1,4-dioxane (16.32 g, 15.8 mL) were added into a 50 mL flask with a magnetic bar. 1,3,5-Trioxane (0.56 g, 6.24 mmol) was also added into the flask as an internal reference for determination of the monomer conversion by ^{1}H NMR. The solution in the septum-sealed flask was purged for 30 min with nitrogen and then heated to 80 °C in a thermostated oil bath under stirring. After 115 min, the polymerization was quenched by rapid cooling upon immersion of the flask in an iced water bath. The overall monomer molar conversion (68%) was determined by ^{1}H NMR spectroscopy in $CDCl_3$ by the relative integration of the protons of 1,3,5-trioxane at 5.0 ppm and the vinylic protons of monomers at 5.5 and 6.0 ppm. The polymer was purified by two precipitation/filtration cycles in diethyl ether at 15 °C and dried in a vacuum oven at room temperature. After methylation of the carboxylic acid groups,[49] it was further analyzed by SEC in THF (experimental M_n: M_n^{LS} = 11 700 g/mol; M_w/M_n (PS calibration) = 1.08; dn/dc = 0.069 mL/g).

***In Situ* Synthesis of P(MAA-*co*-PEO_8MA)-*b*-polystyrene Amphiphilic Diblock Copolymers Self-Assemblies by Aqueous Emulsion Polymerization.** The experimental conditions are detailed in Tables 1 and 2. In a typical experiment (entry 8, Table 2), the polymerization of styrene (1.247 g, 12 mmol) was carried out with P(MAA-*co*-PEO_8MA)-TTC (M_n = 15 000 g/mol, 0.463 g, 0.03 mmol), a water-soluble radical initiator ACPA (1.7 mg, 0.006 mmol), and $NaHCO_3$ (1.6 mg, 0.019 mmol) in 5.0 mL of water. A 1 N solution of NaOH (0.07 g) was added to adjust the pH at 5. The solution was placed in a septum-sealed flask, purged for 30 min with nitrogen in an ice bath, and heated at 80 °C in a thermostated oil bath under stirring. The polymerization was finally quenched after 22 h by immersion of the flask in iced water. The monomer conversion was determined by gravimetry. After drying and subsequent methylation of the COOH groups,[49] the polymer was analyzed by SEC in THF solution, and M_n was derived from the light scattering (LS) response, while M_w/M_n was calculated with a calibration curve based on polystyrene standards. The refractive index increment (dn/dc = ν) for well-defined diblock copolymers was calculated according to dn/dc = $w_A\nu_A + w_B\nu_B$, where w is the weight fraction of P(MAA-*co*-PEO_8MA)-TTC (A with ν_A = 0.064) and polystyrene (B with ν_B = 0.185), respectively[50] (see Table SI-1 in the Supporting Information).

***In Situ* Synthesis of P(MAA-*co*-$PEO_{19}MA$)-*b*-polystyrene Amphiphilic Diblock Copolymers Self-Assemblies by Aqueous Emulsion Polymerization.** The experimental conditions are

Table 1. Aqueous Emulsion Polymerization of Styrene (S) at 80 °C in the Presence of P(MAA-*co*-PEO$_8$MA)-TTC (50:50 mol:mol; M_n = 15 kg mol^{-1}; PDI = 1.16) at a Concentration of 6 mM$_{H_2O}$ at Different pH ([S]$_0$ = 1.2 M$_{H_2O}$, [S]$_0$/[MacroRAFT]$_0$ = 200, [NaHCO$_3$]$_0$ = 4 mM$_{H_2O}$, [ACPA]$_0$ = 1.2 mM$_{H_2O}$; Reaction Time = 22 h)[a]

no.	pH	conv (%)	τ[b] (wt %)	M_n^{th}[c] (kg/mol)	M_n^{PS}[d] (kg/mol)	PDI[d]	M_n^{LS}[e] (kg/mol)
1	3	93	17	34.7	20.5	1.82[f]	
2	5	94	17	35.3	21.4	1.35	36.2
3	6	72	15	30.0	18.3	1.27	32.5
4	8	78	16	30.8	17.1	1.48[g]	33.0

[a] All concentrations (or apparent concentration for styrene) are given on the basis of the amount of water in the system. [b] Final solids content in wt % based on the overall weight of latex. [c] Theoretical M_n calculated at the measured experimental conversion. [d] M_n = number-average molar mass and PDI = M_w/M_n, determined by SEC in THF with a PS calibration (M_n values have been recalculated to notify the non-methylated mass of the polymer). [e] Number-average molar mass determined by SEC in THF equipped with a static light scattering (LS) detector (M_n values have been recalculated to notify the non-methylated mass of the polymer). [f] Multiple populations. [g] Residual P(MAA-*co*-PEO$_8$MA)-TTC.

Table 2. Aqueous Emulsion Polymerization of Styrene (S) in the Presence of P(MAA-*co*-PEO$_8$MA)-TTC (50:50 mol:mol; M_n = 15.0 kg mol^{-1}; PDI = 1.16) at Various [S]$_0$/[MacroRAFT]$_0$ Ratios (80 °C, pH = 5, [NaHCO$_3$]$_0$ = 4 mM$_{H_2O}$, [ACPA]$_0$ = 1.2 mM$_{H_2O}$)[a]

no.	[S]$_0$ (M$_{H_2O}$)	[S]$_0$/[RAFT]$_0$	[macro RAFT]$_0$ (mM$_{H_2O}$)	conv at 22 h (%)	M_n^{th}[b] (kg/mol)	M_n^{LS}[c] (kg/mol)	PDI[d]	τ[e] (wt %)	main morphology[f]
2	1.2	200	6.0	94	35.3	36.2	1.35	17	s (+ f)
5	1.5	240	6.2	86	36.6	33.8	1.28	19	s (+ f)
6	1.8	290	6.2	97	44.4	41.7	1.18	22	f (+ s)
7[g]	1.8	301	6.0	92	40.6	38.7	1.43	21	v
8	2.4	390	6.2	95	53.8	55.0	1.24	25	v (+ s)
9[g]	2.4	400	6.0	96	51.5	54.6	1.36	24	v
10	3.0	500	6.0	90	61.6	57.4	1.25	27	v
11	6.0	1000	6.0	72	90.2	81.4	1.81	32	v
12	1.2	305	4.0	85	42.0	40.5	1.29	14	f (+ s)
13	1.2	390	3.0	93	52.8	48.9	1.28	14	v

[a] All concentrations (or apparent concentration for styrene) are given on the basis of the amount of water in the system. [b] Theoretical M_n calculated at the measured experimental conversion. [c] Determined by SEC in THF equipped with a LS detection (M_n values have been recalculated to notify the non-methylated mass of the polymer). [d] Determined by SEC in THF with a PS calibration. [e] τ is the final solids contents. [f] Main morphology: s = spheres; f = fibers; v = vesicles. [g] M_n (macroRAFT) = 11.8 kg mol^{-1}; PDI = 1.24.

Table 3. Aqueous Emulsion Polymerization of Styrene (S) in the Presence of P(MAA-*co*-PEO$_{19}$MA)-TTC (50:50 mol:mol; M_n^{LS} = 11.7 kg mol^{-1}; PDI = 1.08) at Various [S]$_0$/[MacroRAFT]$_0$ Ratios (80 °C, pH = 5, [MacroRAFT]$_0$ = 6 mM$_{H_2O}$, [NaHCO$_3$]$_0$ = 4 mM$_{H_2O}$, [ACPA]$_0$ = 1.2 mM$_{H_2O}$)[a]

no.	[S]$_0$ (M$_{H_2O}$)	[S]$_0$/[RAFT]$_0$	t (min)	conv (%)	M_n^{th}[b] (kg/mol)	M_n^{LS}[c] (kg/mol)	PDI[d]	τ[e] (wt %)	main morphology[f]
14	1.5	250	240	100	37.9	41.9	1.20	19	s + f
15	1.8	300	180	93	40.8	45.5	1.20	20	f
16	2.4	400	220	97	52.2	59.8	1.29	24	v

[a] All concentrations (or apparent concentration for styrene) are given on the basis of the amount of water in the system. [b] Theoretical M_n calculated at the measured experimental conversion. [c] Determined by SEC in THF equipped with a LS detection (M_n values have been recalculated to notify the non-methylated mass of the polymer). [d] Determined by SEC in THF with a polystyrene calibration. [e] τ is the final solids contents. [f] Main morphology: s = spheres; f = fibers; v = vesicles.

detailed in Table 3. In a typical experiment (entry 15, Table 3), 0.819 g of P(MAA-*co*-PEO$_{19}$MA)-TTC (M_n = 11 700 g/mol, 0.07 mmol) was dissolved in 10.6 mL of deionized water. Then, 1.3 mL of a stock solution of ACPA in water (concentration of 13.6 g L^{-1} neutralized by 3.5 mol equiv of NaHCO$_3$) and 2.1872 g (21 mmol) of styrene were added. A 1 N solution NaOH (0.14 g) was added to adjust the pH at 5. The solution was placed in a septum-sealed flask, purged for 30 min with nitrogen in an ice bath, and heated at 80 °C in a thermostated oil bath under stirring. The polymerization was finally quenched after 3 h by immersion of the flask in iced water. The monomer conversion was determined by gravimetry. After drying and subsequent methylation of the COOH groups,[49] the polymer was analyzed by SEC in THF solution, and M_n was derived from the light scattering (LS) response, while M_w/M_n was calculated with a calibration curve based on polystyrene standards. The refractive index increment ($dn/dc = \nu$) for well-defined diblock copolymers was calculated according to $dn/dc = w_A\nu_A + w_B\nu_B$, where w is the weight fraction of P(MAA-*co*-PEO$_{19}$MA)-TTC (A with ν_A = 0.069) and polystyrene (B with ν_B = 0.185), respectively (see Table SI-1 in the Supporting Information).

Characterization Techniques. *NMR.* For the macroRAFT agent syntheses, the monomer conversion was determined by ^{1}H NMR spectroscopy (200 or 300 MHz from Bruker) in $CDCl_3$ at room temperature in 5 mm diameter tubes.

dx.doi.org/10.1021/ma2005926 |*Macromolecules* 2011, 44, 4149–4158

SEC. The number-average molar masses (M_n), the weight-average molar masses (M_w) and the molar mass distributions (polydispersity index: PDI = M_w/M_n) were determined by size exclusion chromatography (SEC) using THF as an eluent at a flow rate of 1 mL/min. The carboxylic acid-containing polymers were methylated with trimethylsilyldiazomethane before injection.[49] Two types of SEC apparatus were used in this study: (a) A routine SEC apparatus equipped with a Viscotek VE 5200 automatic injector and two columns (PL gel 5 μm, Mixed-C) thermostated at 40 °C. Detection was made with a differential refractive index detector (Viscotek VE 3580 RI detector). The OmniSEC 4.2 software was used for data analysis, and the relative M_n and M_w/M_n were calculated with a calibration curve based on polystyrene (PS) standards (from Polymer Laboratories), named M_n^{PS}. (b) A more sophisticated apparatus with a triple detector array (TDA, model 302 from Viscotek) equipped with a two angle light scattering (LS) detector (LALS, $\theta = 7°$, RALS, $\theta = 90°$, laser $\lambda = 670$ nm), a refractive index (RI) detector, and three Polymer Laboratories Mixed C columns (5 μm) thermostated at 40 °C (the inline viscosimeter was not used in this work). The number-average molar masses, M_n, were calculated from combined LS and RI signals (M_n^{LS}) with the OmniSEC 4.2 software; the refractive index increment (dn/dc) values of the diblock copolymers were calculated as described above, using the average dn/dc measured for each macroRAFT agent with the inline refractometer injecting polymer at four different concentrations. The reported M_n^{LS} correspond to the calculated non-methylated values. In the plot showing the evolution of M_n with monomer conversion, the straight line corresponds to the expected evolution of the theoretical number-average molar mass, $M_{n,th}$, calculated by the introduced mass of monomer multiplied by conversion divided by the initial mole number of macroRAFT agent plus the molar mass of the latter.

TEM. For transmission electron microscopy (TEM) analyses, samples were dropped on a carbon-coated copper grid and dried under air. The TEM images were recorded without staining using a JEOL JEM 100CX II electron microscope at an accelerating voltage of 100 kV equipped with a 1376 × 1032 pixels CCD camera (Olympus, KeenView). For the experiments 14, 15, and 16, the latexes (diluted suspensions deposited on a Formvar-coated copper grid and evaporated) were examined at an accelerating voltage of 80 kV with a Philips CM120 transmission electron microscope (Centre Technologique des Microstructures (CTμ), University Claude Bernard, Villeurbanne, France).

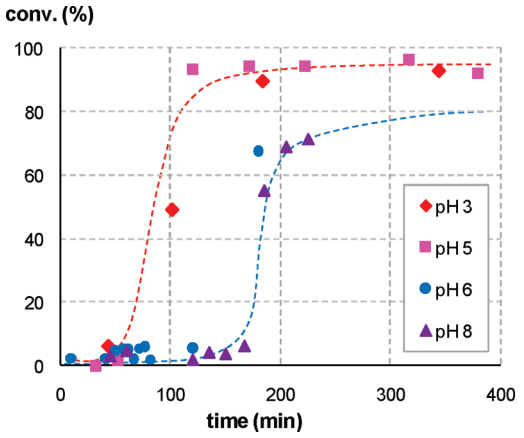

Figure 1. Conversion versus time plot for the emulsion polymerizations of styrene in the presence of P(MAA-*co*-PEO$_8$MA)-TTC macroRAFT agent at different pH (see Table 1).

RESULTS AND DISCUSSION

For the synthesis of the poly(methacrylic acid-*co*-poly(ethylene oxide) methyl ether methacrylate) (P(MAA-*co*-PEOMA)-TTC) macroRAFT agents by random copolymerization of methacrylic acid and poly(ethylene oxide) methyl ether methacrylate (50:50,

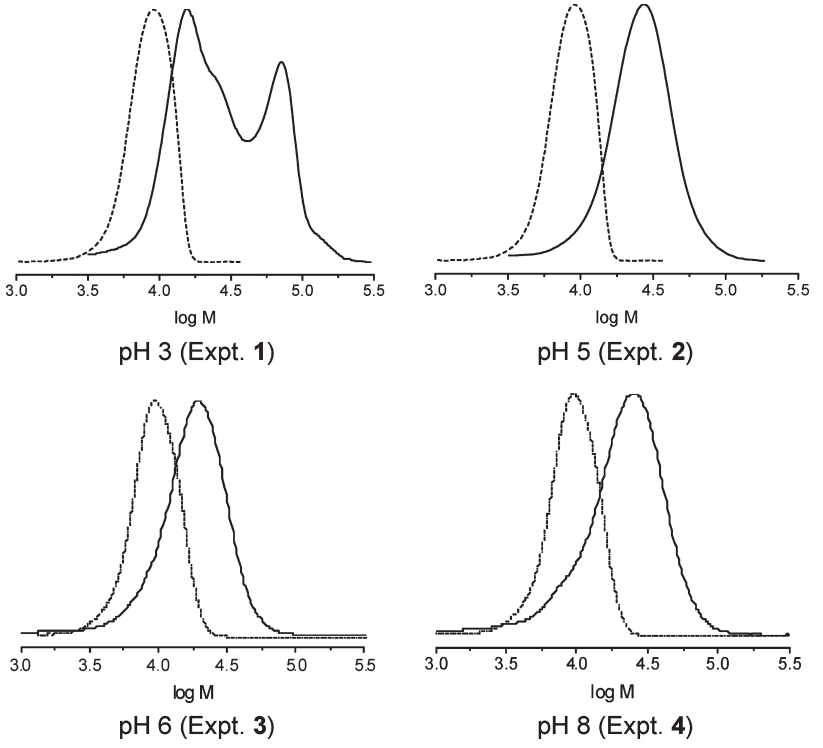

Figure 2. Size exclusion chromatograms (w(log M) vs log M) of P(MAA-*co*-PEO$_8$MA)-TTC (···) and P(MAA-*co*-PEO$_8$MA)-*b*-polystyrene (—) synthesized via aqueous emulsion polymerization of styrene at various pH (see Table 1 for the experimental data).

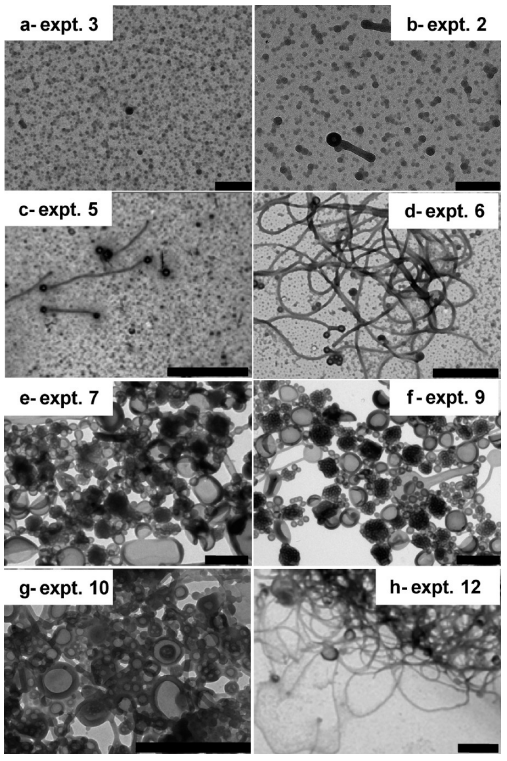

Figure 3. TEM images of the final particles obtained via aqueous emulsion polymerization of styrene using the P(MAA-*co*-PEO_8MA)-TTC macroRAFT agent (see Tables 1 and 2 and the Supporting Information, Figures SI-2, SI-3, and SI-4, for other TEM and scanning electron microscopy images). Scale bars: (a, b) 200 nm; (c−h) 1 μm.

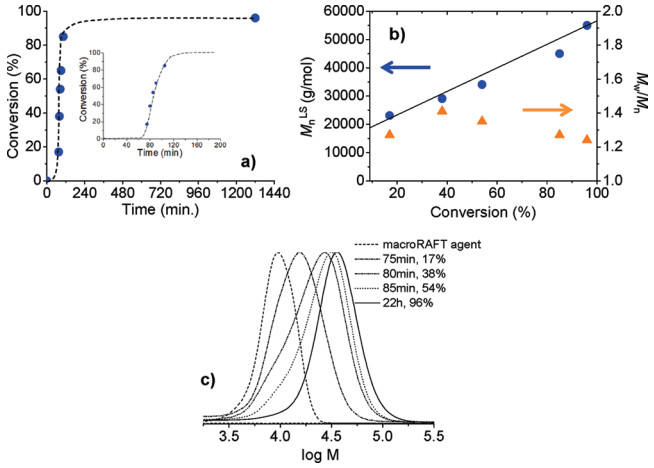

Figure 4. Evolution of the aqueous emulsion polymerization of styrene (experiment 8 in Table 2) with time and monomer conversion. (a) Evolution of the monomer conversion with time (inset: zoom between 0 and 200 min). (b) Evolution of the number-average molar mass (M_n^{LS}, values have been recalculated to designate the non-methylated mass of the polymer) and polydispersity index (M_w/M_n) with monomer conversion. (c) Evolution of SEC traces (w(log M) vs log M) with conversion.

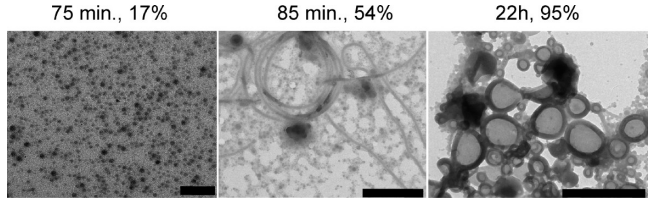

Figure 5. Evolution of the aqueous emulsion polymerization of styrene for experiment 8 (see Table 2): TEM images at different polymerization times and monomer conversions. Scale bars: 75 min: 200 nm; 85 min and 22 h: 1 μm.

mol:mol) in 1,4-dioxane solution, 4-cyano-4-(propylsulfanylthiocarbonyl)sulfanylpentanoic acid (CPP)[47] was chosen as a chain transfer agent. It had indeed proven to be highly efficient in the RAFT-mediated polymerization of methacrylate monomers leading to well-controlled living chains.[47] Two macromonomers with PEO chains of different lengths were used: "PEO_8MA" with an average molar mass, M_n, of 475 g/mol, possessing 8 ethylene oxide units, EO, on average, and "PEO_{19}MA" (M_n = 950 g/mol) exhibiting 19 EO units on average. The initial composition of the monomer mixtures (MAA and PEOMA) was 50:50 mol:mol, and this remained constant throughout the polymerization as determined by ^{1}H NMR and also commented in the literature,[51] indicating negligible compositional drift.

Emulsion Polymerization of Styrene in the Presence of the P(MAA-*co*-PEO_8MA)-TTC Macromolecular RAFT Agent. *Effect of pH.* Targeting the formation of well-defined P(MAA-*co*-PEOMA)-*b*-polystyrene amphiphilic block copolymers via chain extension in an aqueous emulsion polymerization of styrene, we first identified the best pH conditions allowing for the most efficient polymerization control as well as a good colloidal stability. The study was performed with the P(MAA-*co*-PEO_8MA)-TTC macroRAFT agent (see Table 1).

As also observed earlier, significantly faster kinetics and higher final conversions were observed whenever the emulsion polymerization was conducted in acidic conditions, at pH = 3−5 (pK_A PMAA = 5.8[52]) accounting for a faster nucleation step[45,46] (Figure 1). Indeed, in these pH conditions, as shown in Figure 1 (experiments 1 and 2 detailed in Table 1), the polymerization was completed within 2 h, after a short induction period. It is assumed that the induction period corresponds to the time needed to form amphiphilic species with a critical length for the polystyrene hydrophobic block that allows self-assembling and particle formation. Such fast nucleation depends also on the nature of the hydrophilic block and is more favorable in case of low charge density.[45] Indeed, at pH above 6 when the hydrophilic block was increasingly ionized (and in particular for the experiment 4 conducted at pH 8), the induction period was significantly longer, close to 3 h, and complete conversion needed longer time.

Transfer efficiency and quality of control over chain growth were best at pH 5−6, with experimental M_n that matched the theoretical values, low PDIs (experiments 2 and 3 in Table 1) and a complete shift of the size exclusion chromatograms from the macroRAFT agent to the final block copolymer (Figure 2 and Figure SI-2 in the Supporting Information). At pH 3, a loss of control was observed, possibly due to poor water solubility of the macroRAFT agent and partition between the various phases of the system. At pH 8, a small amount of residual macroRAFT agent was observed as a shoulder in the block copolymer SEC peak due to potential hydrolysis of part of the macroRAFT agent and/or an effect of charge density on the quality of nucleation.[45] The very high reinitiation efficiency at pH 5−6 is an important outcome of the polymerization, as a complete

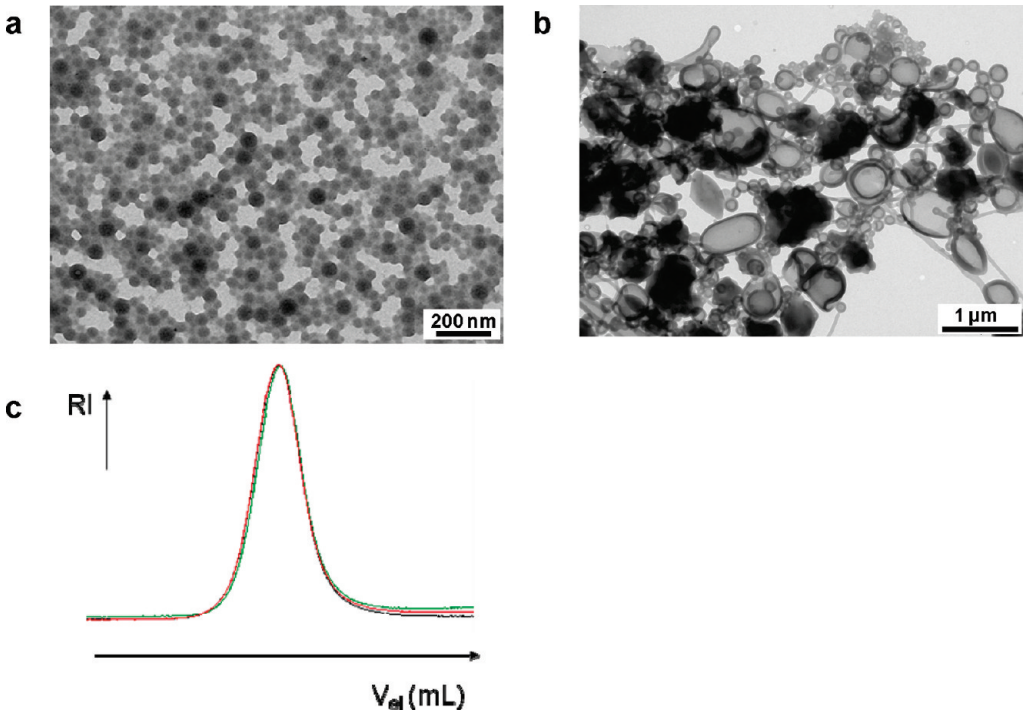

Figure 6. TEM images of experiment 8 (pH 5 with $[S]_0/[\text{macroRAFT}]_0$ ratio = 390) after centrifugation at 3500 rpm for 30 min: (a) supernatant, (b) precipitate. (c) Overlay of the size exclusion chromatograms of the polymer before separation by centrifugation (in red), the supernatant (in black), and the precipitate (in green).

consumption of the macroRAFT agent ensures the absence of free hydrophilic chains in the aqueous phase. Independently of the pH, mainly small spherical micelles were obtained with an average diameter of about 20 nm (Figure 3, experiments 2 and 3, and Figure SI-2 in the Supporting Information).

With P(MAA-*co*-PEO_8MA)-TTC macroRAFT agent, the best experimental conditions to achieve a good control over the macromolecular characteristics of the polymer chains and to reach fast emulsion polymerizations of styrene along with high final conversions were thus those of experiment 2 (Table 1), with a pH of 5.

Effect of the Concentration of Styrene at Constant Macro-RAFT Agent Concentration. A series of experiments were then performed at pH 5, and the polystyrene block length was varied by increasing the initial styrene/macroRAFT molar ratio at constant macroRAFT agent concentration (Table 2, entries 2 and 5−11). This was performed by increasing the initial styrene concentration and had thus the consequence of increasing substantially the polymer content in the final dispersion, from 17 to 32 wt %. In all cases, the dispersions became white, increased in viscosity with the increase in polymer content, and were stable over long periods of time (with only slight sedimentation after a few months). Again, high monomer conversions were reached and independently of the styrene initial concentration, excellent blocking efficiency, and good control over the polymer chain length were observed. The experimental M_n matched the theoretical values, increasing linearly with monomer conversion, and the PDIs were low (Figure 4). These remarkable results stand in contrast to our results obtained earlier for the emulsion polymerization of styrene with the poly(acrylic acid-*co*-poly(ethylene oxide) methyl ether acrylate) trithiocarbonate macroRAFT agents, for which the reinitiation efficiency was lower.[35] The quality of the blocking efficiency with this new methacrylate macroRAFT agent compared to the all-acrylic counterpart must be ascribed to the higher chain transfer constant of the former for styrene polymerization due to the presence of a tertiary radical leaving group.

Transmission electron microscopy (TEM) images (Figure 3; see also the scanning electron microscopy images in Figure SI-3 of the Supporting Information) showed that the morphology of the self-assemblies clearly depended on the hydrophobic block length, for a given length of the macroRAFT agent. Indeed, with increasing hydrophobic block length, a transition from mainly spheres to vesicle-like structures was obtained. Filamentous structures were also observed, but only in a rather narrow window of conditions (for which spherical structures were also present). Such morphology transition with growing length of the hydrophobic block has already been well described when preformed amphiphilic block copolymer were assembled in water using an organic cosolvent for assisting the process.[53]

Consistently, such transitions were also seen when the formation of the nano-objects was monitored during polymerization. At low conversion, i.e., with a short polystyrene block, only small spherical micelles were observed, which transformed into filaments and finally mainly vesicles with growing polystyrene block (Figure 5).

Although a clear relationship was observed between the main morphology and the hydrophobic block length, in most experiments other morphologies were also present in small quantities. For instance, small spheres coexisting in minor quantity besides vesicles in sample 8 could be separated from the vesicles by centrifugation (Figure 6). SEC revealed that both morphologies were composed of chains of the same M_n. Therefore, heterogeneity in morphology cannot be attributed to heterogeneity in

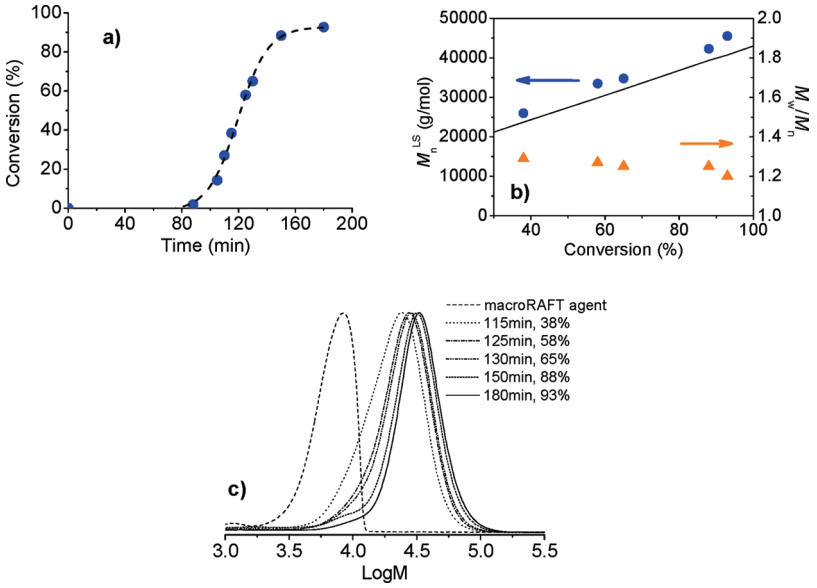

Figure 7. Evolution of the aqueous emulsion polymerization of styrene (experiment 15 in Table 3) with time and monomer conversion. (a) Evolution of the monomer conversion with time. (b) Evolution of the number-average molar mass (M_n^{LS}, values have been recalculated to designate the non-methylated mass of the polymer) and polydispersity (M_w/M_n) with monomer conversion. (c) Evolution of SEC traces ($w(\log M)$ vs $\log M$) with conversion.

polymer chains and vice versa. It might rather be the consequence of the formation mechanism and its kinetics.

Effect of the MacroRAFT Agent Concentration. Three experiments (Table 2, experiments 2, 12, and 13) were performed with the same initial concentration of styrene but different concentrations of macroRAFT agent (6.0, 4.0, and 3.0 mM, respectively). The decrease of the latter, i.e., the concomitant increase in length of the polystyrene block, induced a change in particle morphology from mainly spheres to a mixture of fibers and spheres and finally to vesicle-like objects.

Experiments performed at the same initial styrene/macroRAFT agent ratio but at significantly higher styrene (2.4 M vs 1.2 M) and macroRAFT agent concentrations (8 vs 13 for vesicles and 6 vs 12 for mainly filamentous objects; see Table 2, Figure 3, and Figure 6 for experiment 8 and Figure SI-4 for experiment 13) revealed that the volume of the organic phase had only a negligible impact on the morphology (Figure 3 and Figure SI-4 in the Supporting Information) but that the length of the forming hydrophobic block (determined by the initial styrene/macroRAFT agent ratio) was a key parameter. The effect of monomer concentration stands here in contrast to the observations presented by Li et al.[31] in dispersion polymerization, for which a change in monomer concentration is also accompanied by a change in solvent quality. Such a trend should not be seen in emulsion polymerization where the monomer forms a separate phase and does not impact the solvent quality for the polymer. This result shows also that at a pH of 5 partitioning of the macroRAFT agent in the monomer phase does not seem to play a major role on the outcome of the reaction.

Effect of the MacroRAFT Agent Molar Mass. The influence of the length of the hydrophilic stabilizing P(MAA-*co*-PEO_8MA) block was also investigated: experiments 6 and 7, on the one hand, and experiments 8 and 9 on the other hand (Table 2), were performed in the same conditions but using macroRAFT agents of slightly different M_n (15.0 kg/mol vs 11.8 kg/mol). It appeared that significantly different morphologies were found for the experiments 6 and 7 with a polystyrene block of intermediate length ($DP_{n,PS}$ close to 300), namely fibers (and a minor quantity of spheres) in the case of the longer macroRAFT agent and only vesicles with the shorter one. This is consistent with our earlier study[54] using poly(acrylic acid-*co*-poly(ethylene oxide) methyl ether acrylate) macroRAFT agents, in which we have already found that the length of the macroRAFT agent had an impact on the formed morphology and that shorter ones favored the formation of vesicles or filaments rather than spheres. For both samples 8 and 9 with a longer polystyrene block ($DP_{n,PS}$ close to 400), the difference was however less pronounced and only vesicle-like objects were formed. The change in molar mass of the hydrophilic block is probably too slight here to have an impact and it can be seen only for the experiments 6 and 7 which seem to be at the boundary between different morphologies.

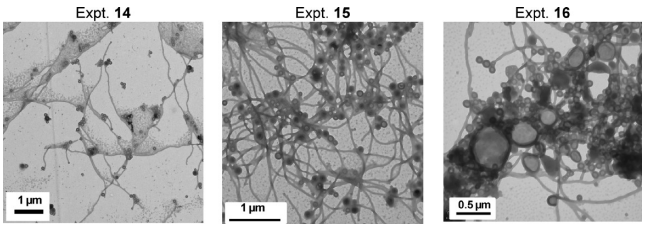

Figure 8. TEM images of the final morphologies obtained via aqueous emulsion polymerization of styrene for the experiments 14−16 performed in the presence of the P(MAA-*co*-PEO_{19}MA)-TTC macroRAFT agent (see Table 3).

Emulsion Polymerization of Styrene in the Presence of the P(MAA-*co*-PEO_{19}MA)-TTC Macromolecular RAFT Agent. A change in the structure of the macroRAFT agent was further studied, namely, a change in the length of the PEO side chains, from 8 EO monomer units (PEO_8MA) to 19 monomer units on average (PEO_{19}MA), while keeping a 50:50 molar ratio of both hydrophilic comonomers.

The experiments 14, 15, and 16 described in Table 3 can be compared with the experiments 5, 6, and 8 in Table 2 (same experimental conditions; different structure and molar mass

dx.doi.org/10.1021/ma2005926 |*Macromolecules* 2011, 44, 4149–4158

of the macroRAFT agents). Again, the polymerizations were well controlled (Figure 7), leading to well-defined amphiphilic diblock copolymers with low polydispersity indices. It appears that the system underwent a change in morphology for the selected range of styrene concentrations (i.e., target polystyrene degrees of polymerization) in a similar way for both systems. This confirms that the target length of the core block is an important parameter for the self-organization of the so-formed amphiphilic diblock copolymers.[41]

Experiment 15 can be directly compared with experiment 7 (same initial concentrations of all compounds, same molar mass of the macroRAFT agent but different lengths of the PEO grafts). It is clear that the morphologies found are not the same. For the experiment 7 performed in the presence of P(MAA-*co*-PEO_8-MA)-TTC, vesicles were formed (Figure 3), whereas mainly filamentous objects were observed for sample 15 (Figure 8). Here, for experiment 7 the overall degree of polymerization of the hydrophilic chain was larger (overall $DP_{n,hydrophilic} = 42$); i.e., the number of grafts was higher while the grafts were shorter, as compared to experiment 15 (overall $DP_{n,hydrophilic} = 22$). The particle morphologies found for the experiments 7 and 15, in comparison also with that of experiment 6, show that the hydrophilic block molar mass and its structure may have opposite effects: fibers are favored over vesicles for short hydrophilic chains with long branches (experiment 15) or longer hydrophilic chains with shorter branches (experiment 6).

DISCUSSION

The system of RAFT-mediated emulsion polymerization of styrene we have developed in this work presents several important advantages: (i) we have chosen polystyrene, a high T_g polymer, as the hydrophobic block, allowing good mechanical stability of the morphologies and the possibility to perform TEM analyses; (ii) the P(MAA-*co*-PEOMA)-TTC macroRAFT agents based on a methacrylate backbone are highly efficient for complete reinitiation and good control over the polymerization of styrene, which is not frequently found in the literature; it allowed well-defined amphiphilic block copolymers to be designed in fast emulsion polymerization systems; (iii) the composition of the macroRAFT agent and the experimental conditions were such that the system was well adjusted to lead to self-assembled amphiphilic block copolymer nanostructures with different morphologies. We have thus in hand a model system to study the previously defined principles of polymerization-induced micellization in water, based on emulsion polymerization,[28−30,32−35] i.e., with monomers that are not initially soluble in the polymerization medium. This is strongly different, in term of mechanism, from aqueous dispersion polymerization, for which the initial system is homogeneous. For the latter, the choice of monomers is rather limited, while in emulsion polymerization all liquid, hydrophobic monomers can be applied. There is thus a great interest in fully understanding the parameters that contribute to a control over the amphiphilic block copolymer self-assemblies when those are formed simultaneously to the hydrophobic chain growth in water.

The parameters we have studied here are the pH, the concentration of styrene, and the concentration, structure, and molar mass of the macroRAFT agents. All of them have an influence. A strong effect was found for the pH, in terms of quality of the polymerization control, and for the styrene/macroRAFT agent ratio (i.e., target chain length of the hydrophobic block) in terms of morphology of the formed nano-objects. By comparison, a slight change in the molar mass of the macroRAFT agent and its structure had an effect only within the appropriate window of polystyrene chain length. The effects of those parameters are depicted in Figure 9, where it appears clearly that long target polystyrene blocks (i.e., high styrene concentration and/or low macroRAFT agent concentration) lead to vesicle-like objects, whereas short target polystyrene blocks favor the formation of spheres. Only a narrow window of concentrations promotes the formation of nanofibers.

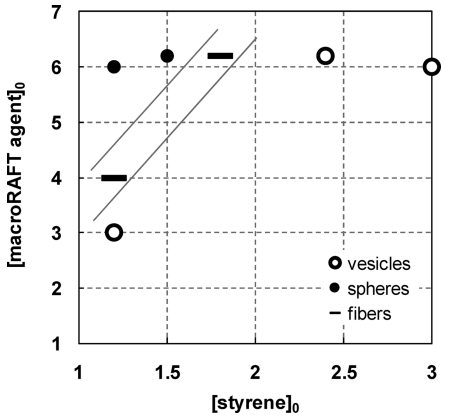

Figure 9. Representation, in a concentration diagram, of the nano-object main morphologies observed for the aqueous emulsion polymerizations of styrene performed in the presence of P(MAA-*co*-PEO_8MA)-TTC (50:50 mol:mol; M_n = 15.0 kg mol^{-1}; PDI = 1.16) at pH 5 (experiments 2, 5, 6, 8, 10, 12, and 13 in Table 2). The plain straight lines roughly delimit the domains of morphologies.

All amphiphilic block copolymer chains form in the first stage of the polymerization (although not instantaneously as shown by the shift of SEC peak in Figures 4 and 7) and grow at the same rate of monomer addition (in agreement with the linear variation of M_n with monomer conversion also shown in Figures 4 and 7 and with the same final M_n of the various objects shown in Figure 6). They initially form spherical micelles due to the short hydrophobic block and then change morphology with the increase in the hydrophobic block length and possible coalescence imparted by the insufficient electrostatic stabilization at pH 5 (so-called coagulation/fragmentation mechanism[55]). At intermediate conversion, the monomer, which swells the core, is likely to enhance chain mobility allowing reorganization. Upon consumption of styrene, the aggregates become frozen—as no effect of postpolymerization dilution or pH changes was observed—and the reorganization thus stops (note that polystyrene-based amphiphilic block copolymers are known to form kinetically frozen rather than dynamic micellar aggregates in water[56]). Concerning the formation mechanism, a better understanding was thus permitted by a good control over the polymerization, even though further investigation is still needed to reach a more complete picture.

CONCLUSION

We report here the use of water-soluble macroRAFT agents in the emulsion polymerization of styrene allowing for the first time fast polymerizations and high final conversions to be achieved along with the formation of well-defined amphiphilic block copolymers with no residual hydrophilic reactive chains. The

final product is an *in situ* created suspension of self-assembled amphiphilic block copolymer nano-objects, the morphology of which can be tuned by various parameters, in particular the target length of the hydrophobic block. This method provides a significant breakthrough for future applications as it saves time and preparation steps, avoids the presence of organic cosolvent, leads to high solids content suspensions, and may be applied easily at the industrial scale using the traditional units for large tonnage emulsion polymerization.

■ ASSOCIATED CONTENT

Supporting Information. Block copolymer refractive index increments; additional TEM and SEM pictures. This material is available free of charge via the Internet at http://pubs.acs.org.

■ AUTHOR INFORMATION

Corresponding Author

*E-mail: jutta.rieger@upmc.fr (J.R.); bernadette.charleux@lcpp.cpe.fr (B.C.).

■ ACKNOWLEDGMENT

We thank Dongya Liu (LCP) and Thomas Boursier (C2P2) for technical support and Stephan Borensztajn (LISE) for SEM analysis. We are grateful to C′Nano Ile de France for financial support to S. Boissé (PhD scholarship 2007−2010), to the French Ministry of research for W. Zhang's PhD Thesis grant, and to the Agence Nationale de la Recherche (ANR-08-BLAN-0209-01, NAMIS) for financial support to X. Zhang's postdoctoral position. B. Charleux acknowledges the IUF (Institut Universitaire de France) for her nomination as senior member.

■ REFERENCES

(1) Matyjaszewski, K.; Davis, T. P. In *Handbook of Radical Polymerization*; Wiley-Interscience: Hoboken, NJ, 2002.
(2) Braunecker, W. A.; Matyjaszewski, K. *Prog. Polym. Sci.* **2007**, *32*, 93–146.
(3) Barner-Kowollik, C., Ed. *Handbook of RAFT Polymerization*; Wiley-VCH: Weinheim, 2008.
(4) Matyjaszewski, K., Gnanou, Y., Leibler, L., Eds. *Macromolecular Engineering: Precise Synthesis, Materials Properties, Applications*; Wiley-VCH: Weinheim, 2007; Vol. 1.
(5) Jenkins, A. D.; Jones, R. G.; Moad, G. *Pure Appl. Chem.* **2010**, *82*, 483–491.
(6) Qiu, J.; Charleux, B.; Matyjaszewski, K. *Prog. Polym. Sci.* **2001**, *26*, 2083–2134.
(7) Monteiro, M.; Charleux, B. In *Chemistry and Technology of Emulsion Polymerisation*; van Herk, A., Ed.; Blackwell Publishing Ltd.: Oxford, 2005; Chapter 5, pp 111−139.
(8) Save, M.; Guillaneuf, Y.; Gilbert, R. G. *Aust. J. Chem.* **2006**, *59*, 693–711.
(9) McLeary, J. B.; Klumperman, B. *Soft Matter* **2006**, *2*, 45–53.
(10) Cunningham, M. F. *Prog. Polym. Sci.* **2008**, *33*, 365–398.
(11) Zetterlund, P. B.; Kagawa, Y.; Okubo, M. *Chem. Rev.* **2008**, *108*, 3747–3794.
(12) Charleux, B.; Nicolas, J. *Polymer* **2007**, *48*, 5813–5833.
(13) Charleux, B.; D'Agosto, F.; Delaittre, G. *Adv. Polym. Sci.* **2010**, *233*, 125–183.
(14) Kagawa, Y.; Minami, H.; Okubo, M.; Zhou, J. *Polymer* **2005**, *46*, 1045–1049.
(15) Nicolas, J.; Ruzette, A. V.; Farcet, C.; Gérard, P.; Magnet, S.; Charleux, B. *Polymer* **2007**, *48*, 7029–7040.
(16) Airaud, C.; Héroguez, V.; Gnanou, Y. *Macromolecules* **2008**, *41*, 3015–3022.
(17) Airaud, C.; Ibarboure, E.; Gaillard, C.; Héroguez, V. *J. Polym. Sci., Part A* **2009**, *47*, 4014–4027.
(18) Ferguson, C. J.; Hughes, R. J.; Pham, B. T. T.; Hawkett, B. S.; Gilbert, R. G.; Serelis, A. K.; Such, C. H. *Macromolecules* **2002**, *25*, 9243–9245.
(19) Ferguson, C. J.; Hughes, R. J.; Nguyen, D.; Pham, B. T. T.; Gilbert, R. G.; Serelis, A. K.; Such, C. H.; Hawkett, B. S. *Macromolecules* **2005**, *38*, 2191–2204.
(20) Manguian, M.; Save, M.; Charleux, B. *Macromol. Rapid Commun.* **2006**, *27*, 399–404.
(21) Sprong, E.; Leswin, J. S. K.; Lamb, D. J.; Ferguson, C. J.; Hawkett, B. S.; Pham, B. T. T.; Nguyen, D.; Such, C. H.; Serelis, A. K.; Gilbert, R. G. *Macromol. Symp.* **2006**, *231*, 84–93.
(22) Delaittre, G.; Nicolas, J.; Lefay, C.; Save, M.; Charleux, B. *Chem. Commun.* **2005**, 615–616.
(23) Delaittre, G.; Nicolas, J.; Lefay, C.; Save, M.; Charleux, B. *Soft Matter* **2006**, *2*, 223–231.
(24) Delaittre, G.; Save, M.; Charleux, B. *Macromol. Rapid Commun.* **2007**, *28*, 1528–1533.
(25) Delaittre, G.; Charleux, B. *Macromolecules* **2008**, *41*, 2361–2367.
(26) Božović-Vukić, J.; Mañon, H. T.; Meuldijk, J.; Koning, C.; Klumperman, B. *Macromolecules* **2007**, *40*, 7132–7139.
(27) Bathfield, M.; D'Agosto, F.; Spitz, R.; Charreyre, M. T.; Pichot, C.; Delair, T. *Macromol. Rapid Commun.* **2007**, *28*, 1540–1545.
(28) Dire, C.; Magnet, S.; Couvreur, L.; Charleux, B. *Macromolecules* **2009**, *42*, 95–103.
(29) Brusseau, S.; Belleney, J.; Magnet, S.; Couvreur, L.; Charleux, B. *Polym. Chem.* **2010**, *1*, 720–729.
(30) Delaittre, G.; Dire, C.; Rieger, J.; Putaux, J.-L.; Charleux, B. *Chem. Commun.* **2009**, 2887–2889.
(31) Li, Y.; Armes, S. P. *Angew. Chem., Int. Ed.* **2010**, *49*, 4042–4046.
(32) Rieger, J.; Stoffelbach, F.; Bui, C.; Alaimo, D.; Jérôme, C.; Charleux, B. *Macromolecules* **2008**, *41*, 4065–4068.
(33) Rieger, J.; Osterwinter, G.; Bui, C.; Stoffelbach, F.; Charleux, B. *Macromolecules* **2009**, *42*, 5518–5525.
(34) Rieger, J.; Zhang, W.; Stoffelbach, F.; Charleux, B. *Macromolecules* **2010**, *43*, 6302–6310.
(35) Boissé, S.; Rieger, J.; Belal, K.; Di-Cicco, A.; Beaunier, P.; Li, M.-H.; Charleux, B. *Chem. Commun.* **2010**, *46*, 1950–1952.
(36) Yeole, N.; Hundiwale, D.; Jana, T. *J. Colloid Interface Sci.* **2011**, *354*, 506–510.
(37) Discher, D. E.; Eisenberg, A. *Science* **2002**, *297*, 967–973.
(38) Blanazs, A.; Armes, S. P.; Ryan, A. J. *Macromol. Rapid Commun.* **2009**, *30*, 267–277.
(39) Yan, X. H. *J. Am. Chem. Soc.* **2004**, *126*, 10059–10066.
(40) Discher, D. E.; Ortiz, V.; Srinivas, G.; Klein, M. L.; Kim, Y.; Christian, D.; Cai, S.; Photos, P.; Ahmed, F. *Prog. Polym. Sci.* **2007**, *32*, 838–587.
(41) Zhulina, E. B.; Adam, M.; LaRue, I.; Sheiko, S. S.; Rubinstein, M. *Macromolecules* **2005**, *38*, 5330–5351.
(42) Wan, W.-M.; Sun, X.-L.; Pan, C.-Y. *Macromolecules* **2009**, *42*, 4950–4952.
(43) Wan, W.-M.; Hong, C.-Y.; Pan, C.-Y. *Chem. Commun.* **2009**, 5883–5885.
(44) Wan, W.-M.; Sun, X.-L.; Pan, C.-Y. *Macromol. Rapid Commun.* **2010**, *31*, 399–404.
(45) Wang, X.; Luo, Y.; Li, B.; Zhu, S. *Macromolecules* **2009**, *42*, 6414–6421.
(46) Luo, Y.; Wang, X.; Li, B.-G.; Zhu, S. *Macromolecules* **2011**, *44*, 221–229.
(47) Xu, X.; Smith, A. E.; Kirkland, S. E.; McCormick, C. L. *Macromolecules* **2008**, *41*, 8429–8435.
(48) Boursier, T.; Chaduc, I.; Rieger, J.; D'Agosto, F.; Lansalot, M.; Charleux, B. *Polym. Chem.* **2011**, *2*, 355–362.
(49) Couvreur, L.; Charleux, B.; Guerret, O.; Magnet, S. *Macromol. Chem. Phys.* **2003**, *204*, 2055–2063.

(50) *Polymer Handbook*, 4th ed.; Brandrup, J., Immergut, E. H., Grulke, E. A., Eds.; Wiley-Interscience: New York, 1999; p VII/548.
(51) Rinaldi, D.; Hamaide, T.; Graillat, C.; D'Agosto, F.; Spitz, R.; Georges, S.; Mosquet, M.; Maitrasse, P. *J. Polym. Sci., Part A: Polym. Chem.* **2009**, *47*, 3045–3055.
(52) Fernyhough, C.; Ryan, A. J.; Battaglia, G. *Soft Matter* **2009**, *8*, 1674–1682.
(53) Zhang, L.; Eisenberg, A. *Science* **1995**, *268*, 1728–1731.
(54) Boissé, S. PhD Thesis Dissertation, University Pierre and Marie Curie, Paris 6, France, 2010; pp 167−169.
(55) Denkova, A. G.; Mendes, E.; Coppens, M.-O. *Soft Matter* **2010**, *6*, 2351–2357.
(56) Nicolai, T.; Colombani, O.; Chassenieux, C. *Soft Matter* **2010**, *6*, 3111–3118.